

The centriolar cartwheel structure: symmetric, stacked, and polarized.

Ioannis Vakonakis^{1,2}

1) Department of Biochemistry, University of Oxford, Oxford OX1 3QU, United Kingdom

2) Correspondence e-mail: ioannis.vakonakis@bioch.ox.ac.uk; Tel.: +44 1865 275725

Highlights

- Cartwheels have 9-fold radial symmetry deriving from ring-shaped SAS-6 oligomers.
- SAS-6 rings stack with average periodicity of ~4 nm into cartwheels.
- A cartwheel inner density (CID) is found in centrioles from diverse species.
- Offsets in SAS-6 ring stacking and CID binding suggest cartwheels are polarized.
- The height of cartwheels is set by two negative feedback loops.

Abstract

An accurate centriolar structure is crucial for organelle function, necessitating the existence of molecular mechanisms for the tight control of centriole assembly. Formation of an initial scaffold, the cartwheel, assists the correct placement of centriolar proteins during assembly and templates key structural parameters of the organelle. Past work illustrated how cartwheel and centriolar symmetry are linked, and grounded organelle symmetry and diameter to the properties of the centriolar protein SAS-6. However, questions remained over how centriole polarity and length are controlled. Recent advances in resolving cartwheel structure and cell biology showed that these assemblies are polarized and that their length is under the control of a homeostatic mechanism. These cartwheel properties may, in turn, influence the centriolar polarity and length.

Introduction

Centriolar structure, reviewed extensively elsewhere in this issue, combines an extraordinary balance between complexity of features and simplicity of built. On one hand, centrioles are among the largest protein-based assemblies in cells, $\sim 0.5\ \mu\text{m}$ -long and $\sim 250\ \text{nm}$ in diameter in most species, with well-defined structural properties. Centrioles are cylindrical in shape defined by an exterior microtubule-based wall, and possess near-universal 9-fold radial symmetry and axial polarity that distinguishes proximal and distal cylinder ends. On the other hand, extensive genetic and molecular studies identified only a handful of protein components necessary for starting to build these organelles and for defining their architecture. Thus, nature has successfully addressed the problem of how to create a very complex structure from few building blocks.

A key step for achieving this organisational feat is the formation of a protein scaffold, the cartwheel, early in the organelle assembly process [1]. Cartwheels work in concert with downstream centriolar components, such as microtubules and connecting proteins [2], to define centriolar radial symmetry and polarity. In so doing, cartwheels narrow the possible building parameters of centrioles and stabilize intermediates of the building process [3,4], thereby ensuring that these organelles adopt specific and consistent structural properties. Conversely, cells that cannot form cartwheels either do not assemble centrioles in their vast majority, or create organelles that are often disjointed, broken up or with altered architecture [5]. As errors in centriole assembly can directly lead to genetic instability, developmental dysfunctions and ciliopathies [reviewed in [6], cartwheel scaffolds are, thus, partly responsible for ensuring cellular and organism health. This short review aims to illustrate recent advancements on understanding the structure of cartwheels and on how this structure links to the centriole architecture.

The cartwheel hub-and-spokes architecture is linked to centriolar radial symmetry and diameter

Cartwheels are 9-fold radially symmetric assemblies already observed by electron microscopy of centrioles over 60 years ago [7]. In top-down views of the centriolar cylinder, cartwheels, occupying the centre of the proximal end of the cylinder, show a $\sim 23\ \text{nm}$ diameter circular hub from which thin spoke protrusions emanate towards the centriole periphery (Fig. 1A). This top wheel-like view of a hub decorated with spokes inspired the cartwheel name and is consistent across all species studied thus far, from humans [8] to green algae [1], with the exception of nematodes, where a central tube scaffold was observed instead [3].

The cartwheel hub-and-spoke architecture is grounded in the properties of a single, essential centriolar protein, spindle assembly abnormal 6 (SAS-6) [9,10]. The SAS-6 molecular architecture is universally conserved and comprises a globular head domain at the N-terminus, a two-stranded,

parallel coiled-coil domain at its centre and a disordered C-terminal tail (Fig. 1B) [11-13]. Crystallographic, electron microscopy and atomic-force microscopy studies showed that SAS-6 from diverse species forms dimers via the coiled-coil domain of this protein, which then rapidly multimerize (in just over 100 seconds, on average [14]) through self-association interactions at the head domain (Fig. 1B) into 9-fold symmetric assemblies (Fig. 1C) [4,11-13,15-17]. In these assemblies, SAS-6 head domains formed a closed ring of size and appearance equivalent to the cartwheel hub, while the 42-50 nm-long SAS-6 coiled coils projected outwards in a radial fashion similar to cartwheel spokes (Fig. 1D). Thus, the shape of SAS-6 multimers directly accounts for the cartwheel hub-and-spoke appearance, while the dimensions of the SAS-6 ring and coiled coils influence the cartwheel diameter and, thus, the positioning of downstream centriolar components. The close connection between SAS-6 multimerization and the cartwheel architecture was underlined in studies of SAS-6 variants, where engineered mutations caused SAS-6 to form multimers with altered radial symmetry and which in turn gave rise to non-9-fold symmetric cartwheels [18]. Whereas loss of cartwheels de-stabilized the centriole architecture so that organelles of aberrant symmetry could form [5], assembly of cartwheels with lower (<9-fold) radial symmetry actively ‘pushed’ centrioles to 8-fold symmetric construction [18]. Thus, a direct link exists between the symmetry of cartwheels and that of centrioles.

Cartwheel stacking and the emergence of centriole polarity

Longitudinal views of cartwheels revealed early on a laminar structure of multiple stacked layers [7] that were later thought to correspond to SAS-6 multimers, each one of which is ~4 nm thick at its central ring [11,12,17]. Cryo-electron tomography of purified *Trichonympha* spp. centrioles at ~40 Å resolution originally suggested that stacking periodicity at the cartwheel hub was 8.5 nm; thus, that SAS-6 rings do not directly contact each other in the stack [19,20]. However, more recent electron tomography data of up to ~24 Å resolution from purified *Trichonympha* spp., *T. agilis*, *Teranympha mirabilis*, *Paramecium tetraurelia*, *Naegleria gruberi* and human centrioles [8,21], as well as *in situ* tomography of *Chlamydomonas reinhardtii* cell sections [8], altered our view of cartwheel stacking.

In these more recent studies, the basic building block of cartwheels was a pair of SAS-6 rings in close contact, spaced ~3.5 nm apart (Fig. 2A,B). While such tight spacing is physically possible, it creates restrictions on the relative placement of rings that may be relevant for cartwheel function (see below). Each pair of SAS-6 rings was complemented by a single, donut-shaped continuous electron density located at the SAS-6 ring interior, referred to as cartwheel inner density (CID; Fig. 2A-C). CIDs were first observed in *Trichonympha* centrioles and thought to be specific to the exceptionally long organelles of this genus that feature cartwheels up to ~4 µm in height [19]; however, CIDs have now also been observed in human, *Chlamydomonas*, *Paramecium* and *Naegleria* centrioles that feature

short cartwheels of ~150 nm height on average [8], suggesting that CIDs perform a conserved but unknown function. Cartwheels from *Teranympha*, another termite gut symbiont with long centrioles, lacked CIDs but featured a filamentous density at their centre; it remains unclear whether and how CIDs and these filaments are related. On the basis of crystallographic structures SAS-6 cannot account for the presence of such densities in the cartwheel interior (Fig. 2C), and CIDs were not seen in cartwheel-like assemblies formed *in vitro* using recombinant *Chlamydomonas* SAS-6 [21,22], or in SAS-6 rings formed by purified human [4], zebrafish [11] or *Leishmania* [17] proteins. This suggests that CIDs and filaments correspond to one or more yet-unidentified centriolar components.

In most cartwheels studied, pairs of SAS-6 rings were stacked ~5 nm apart, thereby creating an average vertical periodicity at the cartwheel hub of ~4.2 nm [8,21]. It is worth noting that this matches the spacings of cartwheels reconstituted *in vitro* by *Chlamydomonas* SAS-6 [21] and suggests that stacking is an inherent property of SAS-6 rings. Combined, the spacings within and between SAS-6 ring pairs give rise to 8.0-8.7 nm cartwheel periodicity depending on species, as measured for example between successive CIDs or spokes (Fig. 2A). It is interesting to note that this cartwheel periodicity is also reflected in that of microtubule-associated A-C linkers, reported as 8.4-8.6 nm in the tomograms of *Trichonympha*, *Chlamydomonas*, *Paramecium* and *Naegleria* centrioles [8,21], which suggests that the underlying centriolar microtubules may deviate from canonical 8.0 nm spacing. However, uncertainties in these measurements and previous studies reporting canonical microtubule periodicities in e.g. *Chlamydomonas* centrioles [23] render any deviation an open question.

An exception to the rule of stacking SAS-6 ring pairs was noted in *T. agilis* centrioles, where discrete vertical sections of cartwheels featured this type of stacking while in other sections ring pairs and single SAS-6 rings devoid of CID intercalated [21]. The significance of this finding for cartwheel function remains unclear; however, a tentative hypothesis is that while most cartwheels form by stacking of SAS-6 ring pairs, exceptionally long cartwheels such as in *T. agilis* may suffer from structural strain that is released by interposition of single and double SAS-6 rings.

Spokes emanating from stacked SAS-6 rings, corresponding to the dimeric coiled-coil domain of this protein, merge into larger bundles towards the cartwheel periphery; however, details of this merging process vary across organisms, possibly due to the low sequence conservation of the SAS-6 coiled coil. In electron tomography of *Trichonympha* and *Ternympha* centrioles, spokes from two successive SAS-6 ring pairs merged first into binary and then tetrameric bundles (Fig. 2D) [21]. In this fashion, the merging of spokes connected four SAS-6 rings into a ~17 nm-height periodic unit, which matches the vertical spacing of the 'pinhead' structure that connects cartwheels and centriolar microtubules. In contrast, spokes in *Chlamydomonas* and *Paramecium* centrioles merged into hexameric bundles via binary and tetrameric intermediates (Fig. 2E); thus, the periodic unit of those

cartwheels comprises six SAS-6 rings and is ~25 nm long [8]. In contrast to the cartwheel hub, where atomic models can be built by combining crystallographic structures of SAS-6 with tomograms, details of spoke merging remain unclear as we lack high-resolution structures of the relevant SAS-6 coiled-coil segments.

The most surprising revelation in the recent electron tomographic studies was the existence of cartwheel polarity along the centriolar proximal-distal axis [8,21]. Previously, proximal-distal polarity had been observed at the level of centriolar microtubules and structural features directly linked to them, such as pinheads [19,23]. However, it now appears likely that cartwheels provide a fundamental polarity queue at the very beginning of centriole assembly, which may drive directionality of the organelle. Three distinct polar elements in cartwheels have been reported. Firstly, in *Trichonympha* spp. and *T. agilis* centrioles CIDs were consistently offset towards the distal direction by 0.5-1 nm from the centre of the associated SAS-6 ring pair (Fig. 3A) [21]. Second, a tilt angle in spokes of *Trichonympha* and a sub-class of *Teranympha* cartwheels suggested that the pair of SAS-6 rings from which they emanate are not in register but rotated by ~6.5° compared to each other (Fig. 3B) [21], thereby endowing the SAS-6 ring pair with axial polarity [21]. It should be noted that such slight rotation of SAS-6 rings would also relieve steric clashes between SAS-6 N-terminal domains, thus allowing tighter packing of the ring pair. Finally, the angle by which spokes in *Chlamydomonas* and *Paramecium* centrioles emanated from the cartwheel hub and then merged varied along a proximal-distal axis [8]. This variation was most evident in *Paramecium*, where angles from +8° to -18° were observed within each periodic unit of six SAS-6 ring pairs (Fig. 3C). Although these three polarity queue were not observed together in all centriolar cartwheels studied, it is conceivable this was due to limitations in tomographic resolution and specimen preparation or, alternatively, that a subset of these queues may be sufficient to drive organelle polarity. In this latter case, the most important queues are likely to be those defined by cartwheel spokes, as these project towards the organelle exterior where downstream components need to be placed in a polarized manner.

Cartwheel height and the control of centriolar length

As noted above, cartwheel height varies tremendously depending on species, but also up to ~4-fold (40-150 nm) during the cell cycle as shown in *Chlamydomonas* [24]. Indirect evidence, of the longest centrioles (e.g. *Trichonympha*, *Teranympha*) having the tallest cartwheels, suggest a link between these two structural parameters. How cartwheel heights are determined remains only partly understood, but recent studies in *Drosophila melanogaster* embryos and human cells suggested this may be through a homeostatic clock mechanism that affects the amount of SAS-6 recruited for building the cartwheel [25,26].

Previous work demonstrated that polo-like kinase 4 (Plk4), SAS-6, and the essential centriolar proteins STIL in humans or Ana2 in *Drosophila* comprise a core module that controls the onset of centriole duplication [reviewed in [27]. Plk4 interacts directly with STIL / Ana2, which it phosphorylates in a structured pattern [28]. STIL, in turn, enhances Plk4 activity, protects the kinase from degradation, and in its phosphorylated form recruits SAS-6 to a site adjacent to each existing mature centriole. Key for SAS-6 accumulation at a single site per mature centriole (and, hence, for the formation of a single new cartwheel and consequently daughter centriole), but also for controlling the length of time the Plk4-STIL/Ana2-SAS-6 module is active (thus, how tall a cartwheel can be built), are two negative feedback loops. In the first instance, Plk4 controls its own activity by acting as ‘suicide kinase’, whereby Plk4 autophosphorylation triggers its inactivation [25]. In this manner, the amount of phosphorylated STIL able to recruit SAS-6 for cartwheel formation is limited. Second, the STIL-SAS-6 complex accumulated at the site of new centriole assembly acts to negatively regulate Plk4 levels [26], with an effect similar to feedback inhibition mechanisms of enzymes blocked by their own product. Combining two negative feedback loops limiting SAS-6 recruitment can potentially define much more accurately the amount of SAS-6 available for cartwheel assembly, and hence the height of cartwheels.

Conclusions and future perspectives

Over the last decade, cartwheel radial symmetry, the role of SAS-6 in establishing it and how it affects centriolar symmetry have been studied in atomic detail. Recent studies now open the door to understanding the origins of centriolar proximal-distal polarity and potentially length, by suggesting these organelle parameters may also be rooted in cartwheel properties. Thus, resolving how these parameters are defined is a key future pursuit, which will allow us to correlate the structure of this essential scaffold to its function in the centriole organelle. SAS-6 oligomerisation appears crucial for centriole polarity and length, just as it did for centriolar symmetry. However, the roles of STIL/Ana2, and the yet unknown CID components, are likely to be just as important. It is, thus, imperative that we seek to identify the CID proteins, and develop further the already impressive reconstitution attempts of SAS-6 rings and cartwheels [4,11,17,21,22]. Incorporating STIL/Ana2 and CID proteins to SAS-6 scaffolds will bring us closer to the *in vitro* formation of pro-centrioles.

At the same time, we must not forget that nature is tremendously inventive! Indirect evidence point to the existence of non-9-fold symmetric centrioles in some protozoa [29,30], hexapod [31] and fungal species [32], and cartwheel reconstitutions using *Caenorhabditis elegans* SAS-6 revealed an alternative 3D arrangement to that discussed in this review, based on a spiral pattern [16]. Despite this fundamental architectural difference, *C. elegans* SAS-6 oligomers output a canonical 9-fold radial

symmetry and define vertical periodicities compatible with microtubule spacings, showing how powerful yet flexible these molecular arrangements can be.

Conflicts of interest statement

Declaration of interests: none

Acknowledgements

I am grateful to Pierre Gönczy and Paul Guichard for advanced previews of their upcoming manuscripts on centriole electron tomography, and to Roland Sigel for hosting at the University of Zurich.

Figure captions

Figure 1: Cartwheel radial symmetry and the SAS-6 oligomer. (A) Electron micrograph cross-section through a *Pseudotriconympha spp.* centriole, in one of the earliest cartwheel observations. The cartwheel (red dashed circle) is clearly visible. Adapted with permission from [7]. Copyright 1960 Rockefeller University Press. (B) Model from *Chlamydomonas* SAS-6 crystallographic structures [12] showing four copies of the protein joined into coiled-coil dimers that then associate through head to head interactions. (C) SAS-6 ring and spokes model formed by nine dimers of this protein. The outer model diameter varies between species depending on the length of the SAS-6 coiled-coil. (D) Atomic force microscopy image of *Chlamydomonas* SAS-6 rings spontaneously forming on a mica surface. Adapted with permission from [15]. Copyright 2014 American Chemical Society.

Figure 2: Cartwheel stacking and the merging of spokes. (A) Longitudinal cross-section of the *T. agilis* cartwheel cryo-electron tomogram, focusing at the central hub as it appears in the majority class of cartwheels [21]. White stars (shown only on the left-hand side) denote the expected positions of SAS-6 head domains from discrete ring oligomers of this protein. The intensity of electron density along a dashed line (right-hand side) is plotted on the right; note the slight trough that appears at the top of major density peaks, suggesting each corresponds to a pair of SAS-6 rings. Spacings shown are representative values from centriolar tomograms from diverse species [8,21]. (B,C) Fit of a SAS-6 ring pair (modelled from *Chlamydomonas* SAS-6 crystallographic structures [12]) in a section of the *T. agilis* cartwheel hub viewed in two perpendicular orientations. As seen in (C) SAS-6 does not account for the CID. (D,E) Longitudinal cross-sections of the cartwheel tomograms from (D) *Trichonympha spp.* [19] and (E) *Paramecium* [8] showing part of the hub with emanating spokes merging into bundles. White stars denote positions of SAS-6 rings as in (A).

Figure 3: Features of cartwheel proximal-distal polarity. (A) Longitudinal cross-section of the *T. agilis* cartwheel tomogram, showing the distal offset of the CID compared to SAS-6 head domains and

spokes. The values of CID offset are taken from *Trichonympha* spp and *T. agilis* centrioles [21]. White stars denote the expected positions of SAS-6 head domains. (B) Top view of two *Chlamydomonas* SAS-6 rings [12] offset to minimize steric clashes and improve the fit to *Trichonympha* and *Teranympha* cartwheel tomograms [21]. A slight clockwise rotation of the top (distal) ring is necessary for such fit. (C) Longitudinal view of spokes merging in the *Paramecium* centriolar cartwheel [8]. Within the 25 Å periodic unit of this cartwheel, distal spokes merge later and with shallower relative angle compared to proximal spokes.

Figure 4: A homeostatic mechanism controlling cartwheel length. Simplified view of the mechanisms controlling Plk4 activity at the onset of centriole duplication [25,26]. A cascade of phosphorylation reactions triggers accumulation of STIL/Ana2 and its recruitment of SAS-6 assembling into the cartwheel. At the same time Plk4 itself and the STIL/Ana2-SAS-6 complex negatively regulate Plk4 activity, thereby limiting the length of time and/or speed by which cartwheels can form.

References and recommended reading

Papers of particular interest, published within the period of review, have been highlighted as:

*of special interest

** of outstanding interest

1. Cavalier-Smith T: **Basal body and flagellar development during the vegetative cell cycle and the sexual cycle of *Chlamydomonas reinhardtii***. *J Cell Sci* 1974, **16**:529-556.
2. Hiraki M, Nakazawa Y, Kamiya R, Hirono M: **Bld10p constitutes the cartwheel-spoke tip and stabilizes the 9-fold symmetry of the centriole**. *Curr Biol* 2007, **17**:1778-1783.
3. Pelletier L, O'Toole E, Schwager A, Hyman AA, Muller-Reichert T: **Centriole assembly in *Caenorhabditis elegans***. *Nature* 2006, **444**:619-623.
4. *Yoshida S, Tsuchiya Y, Ohta M, Gupta A, Shiratsuchi G, Nozaki Y, Ashikawa T, Fujiwara T, Natsume T, Kanemaki MT, et al.: **HsSAS-6-dependent cartwheel assembly ensures stabilization of centriole intermediates**. *J Cell Sci* 2019, **132**.
Using recombinant human SAS-6, these authors reconstituted ring-like oligomers visualised by electron microscopy. This is the first study to show that human SAS-6 adopts a ring oligomeric architecture.
5. Nakazawa Y, Hiraki M, Kamiya R, Hirono M: **SAS-6 is a cartwheel protein that establishes the 9-fold symmetry of the centriole**. *Curr Biol* 2007, **17**:2169-2174.
6. Nigg EA, Holland AJ: **Once and only once: mechanisms of centriole duplication and their deregulation in disease**. *Nat Rev Mol Cell Biol* 2018, **19**:297-312.
7. Gibbons IR, Grimstone AV: **On flagellar structure in certain flagellates**. *J Biophys Biochem Cytol* 1960, **7**:697-716.
8. **Klena N, Le Guennec M, Tassin AM, van der Hoek H, Erdmann PS, Schaffer M, Geimer S, Aeschlimann G, Kovacic L, Goldie KN, et al.: **The architecture of the centriole cartwheel-containing region revealed by cryo-electron tomography**. *bioRxiv* 2020.07.21.068882 (2020). doi: 10.1101/2020.07.21.068882.
In situ cryo-electron tomography of *Chlamydomonas* centrioles, and tomograms from purified human, *Paramecium* and *Naegleria* organelles, show that SAS-6 rings consistently stack with 4 nm periodicity in cartwheels. CIDs are identified in all species, while the merging of spokes into bundles towards the cartwheel periphery is shown to be axially polarized in *Chlamydomonas* and *Paramecium* centrioles.
9. Leidel S, Delattre M, Cerutti L, Baumer K, Gönczy P: **SAS-6 defines a protein family required for centrosome duplication in *C. elegans* and in human cells**. *Nat Cell Biol* 2005, **7**:115-125.
10. Dammermann A, Muller-Reichert T, Pelletier L, Habermann B, Desai A, Oegema K: **Centriole assembly requires both centriolar and pericentriolar material proteins**. *Dev Cell* 2004, **7**:815-829.
11. van Breugel M, Hirono M, Andreeva A, Yanagisawa HA, Yamaguchi S, Nakazawa Y, Morgner N, Petrovich M, Ebong IO, Robinson CV, et al.: **Structures of SAS-6 suggest its organization in centrioles**. *Science* 2011, **331**:1196-1199.
12. Kitagawa D, Vakonakis I, Olieric N, Hilbert M, Keller D, Olieric V, Bortfeld M, Erat MC, Flückiger I, Gönczy P, et al.: **Structural basis of the 9-fold symmetry of centrioles**. *Cell* 2011, **144**:364-375.
13. Cottee MA, Muschalik N, Johnson S, Leveson J, Raff JW, Lea SM: **The homo-oligomerisation of both Sas-6 and Ana2 is required for efficient centriole assembly in flies**. *Elife* 2015, **4**:e07236.
14. *Nievergelt AP, Banterle N, Andany SH, Gonczy P, Fantner GE: **High-speed photothermal off-resonance atomic force microscopy reveals assembly routes of centriolar scaffold protein SAS-6**. *Nat Nanotechnol* 2018, **13**:696-701.

In this study, atomic force microscopy was used to image the progression of SAS-6 oligomerisation towards rings in near-real time. The authors demonstrated that ring formation can proceed via many different pathways, such as sequential addition of SAS-6 dimers or the joining of shorter oligomers.

15. Pfreundschuh M, Alsteens D, Hilbert M, Steinmetz MO, Muller DJ: **Localizing chemical groups while imaging single native proteins by high-resolution atomic force microscopy.** *Nano Lett* 2014, **14**:2957-2964.
16. Hilbert M, Erat MC, Hachet V, Guichard P, Blank ID, Flückiger I, Slater L, Lowe ED, Hatzopoulos GN, Steinmetz MO, et al.: **Caenorhabditis elegans centriolar protein SAS-6 forms a spiral that is consistent with imparting a ninefold symmetry.** *Proc Natl Acad Sci U S A* 2013, **110**:11373-11378.
17. van Breugel M, Wilcken R, McLaughlin SH, Rutherford TJ, Johnson CM: **Structure of the SAS-6 cartwheel hub from Leishmania major.** *Elife* 2014, **3**:e01812.
18. Hilbert M, Noga A, Frey D, Hamel V, Guichard P, Kraatz SH, Pfreundschuh M, Hosner S, Flückiger I, Jaussi R, et al.: **SAS-6 engineering reveals interdependence between cartwheel and microtubules in determining centriole architecture.** *Nat Cell Biol* 2016, **18**:393-403.
19. Guichard P, Hachet V, Majubu N, Neves A, Demurtas D, Olieric N, Flückiger I, Yamada A, Kihara K, Nishida Y, et al.: **Native architecture of the centriole proximal region reveals features underlying its 9-fold radial symmetry.** *Curr Biol* 2013, **23**:1620-1628.
20. Guichard P, Desfosses A, Maheshwari A, Hachet V, Dietrich C, Brune A, Ishikawa T, Sachse C, Gönczy P: **Cartwheel architecture of Trichonympha basal body.** *Science* 2012, **337**:553.
21. **Nazarov S, Bezler A, Hatzopoulos GN, Nemcikova Villímová V, Demurtas D, La Guennec M, Guichard P, Gönczy P: **Novel features of centriole polarity and cartwheel stacking revealed by cryo-tomography.** *bioRxiv* 2020.07.17.208082 (2020). doi:10.1101/2020.07.17.208082.
Improved resolution (up to 23 Å) cryo-electron tomography of *Trichonympha* centrioles, and new tomograms of *Teranympha* organelles, reveal that the basic building block of cartwheels is a pair of SAS-6 rings. The authors further identify offsets in the positions of CIDs and SAS-6 rings that suggest axial polarity in cartwheels.
22. Guichard P, Hamel V, Le Guennec M, Banterle N, Iacovache I, Nemcikova V, Fluckiger I, Goldie KN, Stahlberg H, Levy D, et al.: **Cell-free reconstitution reveals centriole cartwheel assembly mechanisms.** *Nat Commun* 2017, **8**:14813.
23. *Li S, Fernandez JJ, Marshall WF, Agard DA: **Electron cryo-tomography provides insight into procentriole architecture and assembly mechanism.** *Elife* 2019, **8**.
Cryo-electron tomography of *Chlamydomonas* procentrioles focusing on the microtubule wall and the connection (pinhead) between the wall and cartwheel. A proximal-distal twisting motion is identified in centriolar microtubules, that may be linked to features of cartwheel polarity reviewed here.
24. O'Toole ET, Dutcher SK: **Site-specific basal body duplication in Chlamydomonas.** *Cytoskeleton (Hoboken)* 2014, **71**:108-118.
25. **Aydoğan MG, Wainman A, Saurya S, Steinacker TL, Caballe A, Novak ZA, Baumbach J, Muschalik N, Raff JW: **A homeostatic clock sets daughter centriole size in flies.** *J Cell Biol* 2018, **217**:1233-1248.
Using confocal microscopy, the authors analyze the rate of SAS-6 recruitment during centriole assembly and correlate this to levels of Plk4 activity. They observe that increased Plk4 activity speeds up centriolar growth but also the rate of Plk4 inactivation, thereby acting as a homeostatic mechanism.

26. **Takao D, Watanabe K, Kuroki K, Kitagawa D: **Feedback loops in the Plk4-STIL-HsSAS6 network coordinate site selection for procentriole formation.** *Biol Open* 2019, **8**.
Using live-cell imaging, the authors analyze the levels of human SAS-6, STIL and Plk4 at the site of centriole assembly during the cell cycle, and fit these to a mathematical model. A product inhibition-like negative feedback loop is observed connecting the STIL-SAS-6 complex with Plk4 levels.
27. Arquint C, Nigg EA: **The PLK4-STIL-SAS-6 module at the core of centriole duplication.** *Biochem Soc Trans* 2016, **44**:1253-1263.
28. McLamarrah TA, Buster DW, Galletta BJ, Boese CJ, Ryniawec JM, Hollingsworth NA, Byrnes AE, Brownlee CW, Slep KC, Rusan NM, et al.: **An ordered pattern of Ana2 phosphorylation by Plk4 is required for centriole assembly.** *J Cell Biol* 2018, **217**:1217-1231.
29. Prensier G, Vivier E, Goldstein S, Schrevel J: **Motile flagellum with a "3 + 0" ultrastructure.** *Science* 1980, **207**:1493-1494.
30. Schrevel J, Besse C: **[A functional flagella with a 6 + 0 pattern].** *J Cell Biol* 1975, **66**:492-507.
31. Phillips DM: **Giant centriole formation in *Sciara*.** *J Cell Biol* 1967, **33**:73-92.
32. Riparbelli MG, Dallai R, Mercati D, Bu Y, Callaini G: **Centriole symmetry: a big tale from small organisms.** *Cell Motil Cytoskeleton* 2009, **66**:1100-1105.

Figure 1

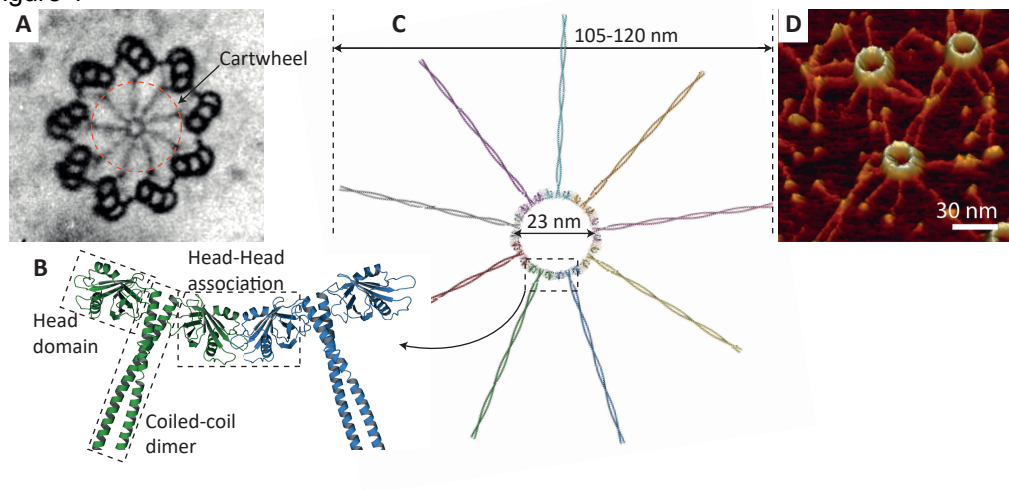


Figure 2

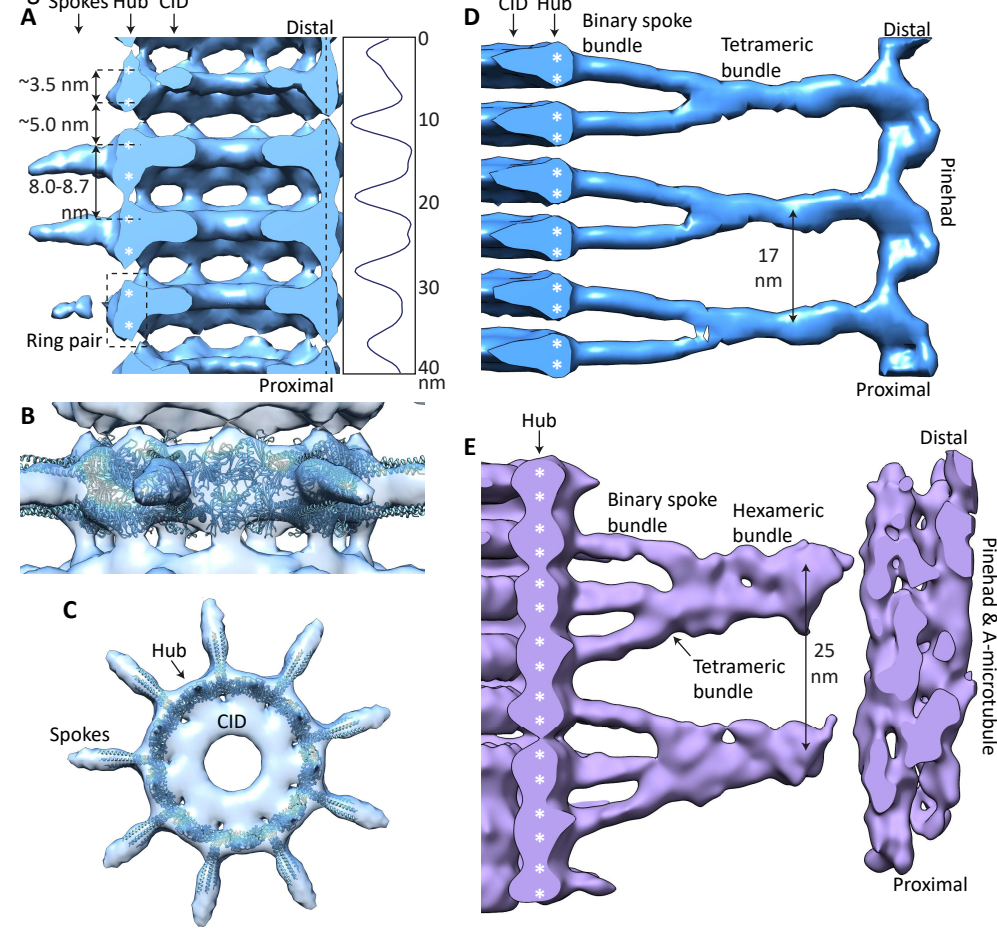


Figure 3

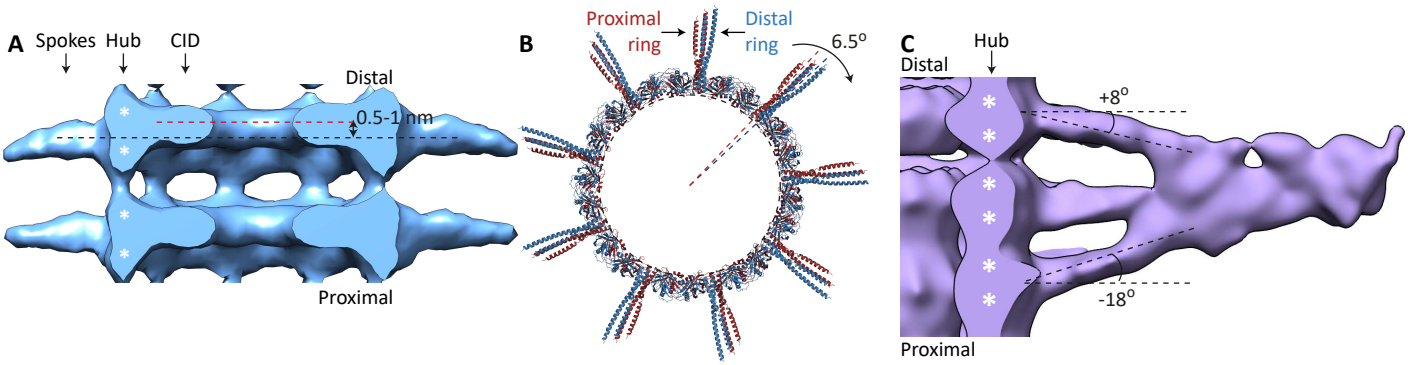


Figure 4

